Coassembling Peptide-Based Biomaterials: Effects of Pairing Equal and Unequal Chain Length Oligopeptides

Sivakumar Ramachandran,[†] Jill Trewhella,[‡,§] Yiider Tseng,[⊥] and Y. Bruce Yu*[,†,#]

Departments of Pharmaceutics & Pharmaceutical Chemistry, Bioengineering, and Chemistry, University of Utah, Salt Lake City, Utah 84112, Department of Chemical Engineering, University of Florida, Gainesville, Florida 32611, and School of Molecular and Microbial Biosciences, University of Sydney, Australia

Received May 8, 2006. Revised Manuscript Received September 17, 2006

We have previously developed shear-responsive hydrogels assembled from mutually attractive but self-repulsive oligopeptide modules. To explore the mechanism of material assembly, we designed and synthesized a quartet of oligopeptides. The peptide quartet contains two positively charged modules 10 and 15 amino acid residues long and two negatively charged modules 10 and 15 amino acid residues long. Each positive module can pair with one negative module and hence there are four potential pairings, two of equal chain length (blunt-ended pairs) and two of unequal chain length (sticky-ended pairs). Viscoelastic properties and structural features of the hydrogels assembled from these oligo-peptide pairs were evaluated by dynamic rheometry and small-angle X-ray scattering (SAXS) techniques, respectively. It was found that the sticky ends provide no advantage in terms of mechanical properties of the hydrogels. Instead, the hydrogel assembled from the 10:10 peptide pair forms the strongest gel. These results are consistent with a cross-β structural model in which β-strands are stacked against each other in a parallel fashion to form nanofibers, the axes of which are perpendicular to individual β-strands. The optimal chain length of oligopeptide modules for such nanofiber network assembly is around 10 amino acid residues.

Introduction

Amino acids are the building blocks of peptides and proteins. Recent advances in protein engineering have envisioned oligopeptides as building blocks for novel supramolecular structures through molecular self-assembly. In fact, natural biomaterials such as collagen ((Gly-Pro-Hpro)$_n$), silk ((Gly-Ala-Gly-Ala-Gly-Ser)$_n$), etc., are simple repeats of oligopeptide sequences that are assembled into supramolecular structures and possess diverse material properties. One approach to mimick molecular self-assembly as seen in nature is to use complementary chemical groups in peptides to facilitate self-assembly.[1] Complementary chemical groups are provided by the different side-chain and/or backbone interactions of oligopeptides, which can involve hydrophobic, ionic, or hydrogen-bonding interactions. Several research groups[2−6] have harnessed this phenomenon to create novel peptide-based biomaterials for various biomedical applications such as tissue engineering[7,8] and biomineralization.[9,10] Our research group has developed a modular design strategy based on mutually attractive but self-repulsive oligopeptide modules. These peptide modules coassemble into a viscoelastic, fibrous network, with fibers having nanoscale dimensions. During the assembly process, they encapsulate about 99 wt % water and are hence called hydrogels. These hydrogels have a repeated shear-responsive property,[11] enabling them to be formulated as injectables. Furthermore, these hydrogels can entrap proteins in their near native state,[12] an essential property for tissue engineering and protein drug-delivery applications. In this current study, we explore another question of molecular design: can sticky ends in the growing fiber facilitate assembly and enhance the bulk material property? Sticky ends, a concept adapted from nucleic acids, in the peptide fibers can be generated by pairing modules of unequal chain lengths in our modular peptide design. The concept of sticky ends has been applied to coiled-coil peptide fibrillogenesis and has been shown to

* Corresponding author. E-mail :bruce.yu@utah.edu. Phone: 801-581-5133. Fax: 801-585-3614.
[†] Department of Pharmaceutics & Pharmaceutical Chemistry, University of Utah.
[‡] Department of Chemistry, University of Utah.
[§] School of Molecular and Microbial Biosciences, University of Sydney.
[⊥] Department of Chemical Engineering, University of Florida.
[#] Department of Bioengineering, University of Utah.

(1) Zhang, S. *Nat. Biotechnol.* **2003**, *21*, 1171−1178.
(2) Petka, W. A.; Harden, J. L.; McGrath, K. P.; Wirtz, D.; Tirrell, D. A. *Science* **1998**, *281*, 389−392.
(3) Aggeli, A.; Bell, M.; Boden, N.; Keen, J. N.; Knowles, P. F.; McLeish, T. C.; Pitkeathly, M.; Radford, S. E. *Nature* **1997**, *386*, 259−262.
(4) Aggeli, A.; Nyrkova, I. A.; Bell, M.; Harding, R.; Carrick, L.; McLeish, T. C.; Semenov, A. N.; Boden, N. *Proc. Natl. Acad. Sci. U.S.A.* **2001**, *98*, 11857−11862.
(5) Mershin, A.; Cook, B.; Kaiser, L.; Zhang, S. *Nat. Biotechnol.* **2005**, *23*, 1379−1380.
(6) Reches, M.; Gazit, E. *Science* **2003**, *300*, 625−627.
(7) Holmes, T. C. *Trends Biotechnol.* **2002**, *20*, 16−21.
(8) Narmoneva, D. A.; Oni, O.; Sieminski, A. L.; Zhang, S.; Gertler, J. P.; Kamm, R. D.; Lee, R. T. *Biomaterials* **2005**, *26*, 4837−4846.
(9) Hartgerink, J. D.; Beniash, E.; Stupp, S. I. *Science* **2001**, *294*, 1684−1688.
(10) Shiba, K.; Honma, T.; Minamisawa, T.; Nishiguchi, K.; Noda, T. *EMBO Rep.* **2003**, *4*, 148−153.
(11) Ramachandran, S.; Tseng, Y.; Yu, Y. B. *Biomacromolecules* **2005**, *6*, 1316−1321.
(12) Ramachandran, S.; Flynn, P.; Tseng, Y.; Yu, Y. B. *Chem. Mater.* **2005**, *17*, 6583−6588.

10.1021/cm061071l CCC: $33.50
Published on Web 11/18/2006

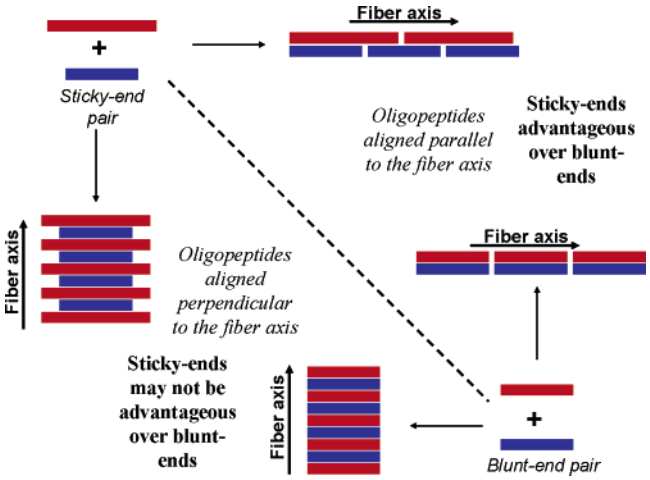

Figure 1. Possible alignment of sticky- and blunt-ended oligopeptides in the nanofiber: perpendicular or parallel orientation of peptide chains with respect to the fiber axis. Sheet conformations are not considered, as they are not supported by electron microscope and SAXS data.

Table 1. Sequences and Possible Pairing of Oligopeptides[a]

Peptide	Sequences of Positively Charged Modules	Possible pairing of peptide modules Blunt-ended pairs
KAW15	Acetyl-KWKAKAKAKAKAKAK-amide	EAW15:KAW15
KAW10	Acetyl-WKAKAKAKAK-amide	EAW10:KAW10
Peptide	**Sequence of a Negatively Charged Module**	**Sticky-ended pairs**
EAW15	Acetyl-WEAEAEAEAEAEAEA-amide	EAW10:KAW15
EAW10	Acetyl-EWEAEAEAEA-amide	EAW15:KAW10

[a] The numbers represent the chain length of peptides. Modular material assembly is achieved by pairing a positive module with a negative module. Positively charged amino acids are in red and negatively charged amino acids are in blue. Peptides with equal and unequal chain lengths were coassembled to create blunt- and sticky-ended pairs, respectively. K, lysine; A, alanine; E, glutamic acid; W, tryptophan.

increase the length and thickness of such fibers.[13] If the peptide strands are oriented along the fiber axis, as observed in coiled-coil fibrillogenesis, then sticky ends could enhance the fibrous network formation and thereby the material property in comparison with the equal chain length pairs. On the other hand, if the peptide strands are oriented perpendicular to the fiber axis, as commonly seen in the cross-β structures of amyloid fibers,[14] then sticky ends may not be advantageous when compared to blunt ends (Figure 1).

A quartet of oligopeptides, with an alternating charged and neutral amino acid sequence pattern,[11] was designed to produce peptide pairs with sticky and blunt ends. The sequences of the positively and negatively charged oligopeptide modules and the possible pairings of oligopeptides are shown in Table 1. Chain lengths of 10 and 15 were chosen, as decapeptides were known to form a viscoelastic hydrogel.[11,12] Alanine was chosen as the neutral amino acid to avoid the low solubility of peptides seen with other hydrophobic amino acids such as valine. N- and C-termini were acetylated and amidated, respectively, to prevent any electrostatic interactions at the peptide terminals, which can complicate data interpretation.

Experimental Methods

Sample Preparation. Oligopeptides were synthesized using Fmoc solid-phase peptide synthesis and purified by reversed-phase HPLC (Agilent Technologies, HP1100 chromatograph system, Wilmington, DE). The mass value for each oligopeptide was verified using MALDI-MS.[11] The purity of the peptides was verified by analytical HPLC. Peptide solutions were dissolved and dialyzed in 50 mM aqueous phosphate buffer at pH 7. The pH of the dialyzed peptide solution was verified and, if necessary, adjusted to pH 7. Concentrations of the peptide solutions were determined on the basis of the molar absorptivity of tryptophan at 280 nm ($\epsilon_{280} = 5690$ M^{-1} cm^{-1}).[15] All the measurements were conducted at a total peptide concentration of 0.25 wt %.

Rheological Characterization. Dynamic rheological measurements were made in a 50 mm cone-and-plate module of a strain-controlled, software-operated rheometer (ARES-100; TA instrument, Piscataway, NJ). The time sweep measurements were conducted at 0.2% strain amplitude and 1 rad/s angular frequency. Repeated shear-induced breakdown-recovery cycles were monitored after breaking the gel with 200% strain.

Small-Angle X-ray Scattering (SAXS). The small-angle X-ray scattering instrument described earlier[16] is now at the University of Utah and was used for measurements at 25 °C. This instrument has a slit geometry, and all analyses were corrected for this. The angular dependence of the scattering of X-rays from particles in a solvent has the form

$$I(Q) = |\langle \int_V (\rho(\vec{r}) - \rho_s) e^{-iQ\cdot\vec{r}}\, d^3r \rangle|^2 \qquad (1)$$

where $\rho(\vec{r})$ is the scattering length density of the scattering particle as a function of atomic position ($\vec{r}$) and ρ_s is the mean scattering length density of the solvent. Q is the momentum transfer vector, having the magnitude $4\pi(\sin\theta)/\lambda$, where 2θ is the scattering angle and λ is the wavelength of the incident X-ray (Cu Kα = 1.54 Å). The integration over the particle volume, V, is rotationally averaged for unoriented particles, and the experiment measures the time and ensemble average for all particles in the sample. The inverse Fourier transform of $I(Q)$ gives the pair distance or vector length distribution function, $P(r)$, for the scattering particle

$$P(r) = \frac{1}{2\pi^2} \int I(Q) Q\cdot r \sin(Q\cdot r) dQ \qquad (2)$$

$P(r)$ can be calculated using indirect Fourier transform methods.[17−19] The r value at which $P(r) = 0$ gives the maximum linear dimension for the scattering particle, d_{max}. The zeroth and second moments of $P(r)$ are the zero angle scattering intensity ($I(0)$) and the radius of gyration of the scattering particle (R_g), respectively. $I(0)$ is proportional to the molecular weight of the scattering particles.

The scattering data were also subjected to both Guinier and mass-fractal analysis. Guinier showed that one can approximate the scattering from rod-shaped particles (i.e., one dimension of the particle is much larger than the other two) in the small Q region as[20]

(13) Pandya, M. J.; Spooner, G. M.; Sunde, M.; Thorpe, J. R.; Rodger, A.; Woolfson, D. N. *Biochemistry* **2000**, *39*, 8728−8734.
(14) Dobson, C. M. *Philos. Trans. R. Soc. London, Ser. B* **2001**, *356*, 133−145.
(15) Gill, S. C.; von Hippel, P. H. *Anal. Biochem.* **1989**, *182*, 319−326.
(16) Heidorn, D. B.; Trewhella, J. *Biochemistry* **1988**, *27*, 909−15.
(17) Svergun, D. I. *J. Appl. Crystallogr.* **1991**, *24*, 485−492.
(18) Svergun, D. I. *J. Appl. Crystallogr.* **1992**, *25*, 495−503.
(19) Svergun, D. I.; Semenyuk, A. V.; Feigin, L. A. *Acta Crystallogr., Sect. A* **1988**, *44*, 244−250.
(20) Guinier, A. *Ann. Phys. (Paris)* **1939**, *12*, 161.

$$QI(Q) = I_c(0)e^{-Q^2R_c^2/2} \quad (3)$$

where R_c is the radius of gyration of cross-section of the rod. $I_c(0)$ is proportional to mass per unit length.

Mass-fractal analysis can be used to analyze materials that have a repetitive mass unit, such as might be anticipated in these hydrogels. The scattering data were fitted to mass-fractal, power-law decay using the following equation[21,22]

$$I(Q) = B_f Q^{-d_f} \quad (4)$$

where, d_f is the fractal dimension of the object and B_f is the power-law scaling prefactor characteristic of the fractal dimensionality of the scattering structure. $d_f = 1$ signifies a stiff rodlike structure and B_f in this case is proportional to the length and fourth power of the diameter of the rod; $d_f = 2$ signifies either a disk- or Guassian-coil-shaped object; $d_f = 1.5$ signifies a swollen Guassian-coil in good solvent. In the case of Guassian-coils ($d_f = 2$ or 1.5), B_f is proportional to the end-to-end distance of the Guassian-coil.[21]

Results and Discussions

Upon mixing, each peptide pair starts to gel, as monitored by dynamic rheometry. The end points in terms of G' of the initial gelation are not very different among the four pairs (Figure 2A). However, the gelation processes are quite different, with that of the EAW10:KAW10 pair being the smoothest and that of the EAW15:KAW15 pair being the most rugged. Repeated shear responsiveness of each of these biomaterials was tested as described earlier.[11] Each of the biomaterials regained their mechanical strength after shear-induced breakdowns. It appears that repeated shear-induced breakdowns acted as a correcting mechanism to repair initial misassembly. Indeed, after 13 cycles of shear-induced breakdowns and recoveries, all four hydrogels have reproducible mechanical properties in the subsequent cycles (Figure 3). Although the initial gelation processes resulted in G' values not far apart from each other (~2−3 fold; Figure 2A), cycles of shear-induced breakdown−recovery resulted in stabilized G' values that are significantly different among the four pairs (~10 fold) with the following order: G'(EAW10:KAW10) > G'(EAW15:KAW10) > G'(EAW10:KAW15) > G'(EAW15:KAW15) (Figure 2B). The conclusion from the rheological measurements is that the EAW10:KAW10 pair forms the strongest gel and the EAW15:KAW15 pair forms the weakest gel, as judged by the stabilized G' value.

Transmission electron microscopic (TEM) images of all hydrogels show the formation of fibrous network (see Figure S1 of Supporting Information). However, the drying step involved in the sample preparation for TEM might cause peptide fibers to aggregate further, giving rise to very heterogeneous samples that were difficult to characterize accurately in terms of fiber thickness,[23] estimated very approximately as ~30 nm (diameter). We therefore turned to small-angle X-ray scattering (SAXS) to probe the hydrated fibrous network with minimal perturbations to the samples. The measured scattering intensity ($I(Q)$) increased over time for each of the biomaterials, indicative of the formation of aggregates and consistent with a growing fibril networks (Figure 4). Each of the peptide pairs shows evidence for the development of structures having long-range order that gives rise to small-angle scattering profiles that reached equilibrium over approximately a 24-hour period. The trend of the gelation kinetics is evident in Figure 4 and in the summary of the structural parameters that can be determined using $P(r)$ analysis[16] (Table 2). The kinetics of the formation of these structures is distinctive among the peptide pairs, with the EAW15:KAW15 pair reaching equilibrium most rapidly (between 15 min and 1 h) and the EAW10:KAW10 pair taking more than 11 h before its small-angle scattering pattern becomes evident. The overall gelation kinetics monitored by SAXS follows a clear order of EAW15:KAW15 > EAW10:KAW15 > EAW15:KAW10 > EAW10:KAW10. The order of gelation kinetics can be directly correlated to the total electrostatic and hydrophobic interactions among the oligopeptide pairs, which is highest for the EAW15:KAW15 pair and least for the EAW10:KAW10 pair. Among the two unequal chain length pairs, the kinetics of EAW10:KAW15 (13 charged and 12 apolar amino acids) was faster than that of EAW15:KAW10 (12 charged and 13 apolar amino acids). This difference in gelation kinetics might be attributed to higher electrostatic interactions (longer-range) in the former.

Table 2 summarizes the structural parameters derived from $P(r)$ analysis of the SAXS data at two time points: 11 and 24 h. It should be noted that the maximum dimensions (d_{max}) of the structures within the hydrogel materials are near, and for the largest structures are beyond, the limit of what can be measured accurately given the minimum Q value (Q_{min} = 0.0054 Å^{-1}) measured in these experiments. Thus the larger d_{max} values should be viewed as lower limits. The average dimensions of structural features within each hydrogel reveal that the two peptide pairs containing KAW15 gave rise to scattering patterns indicative of larger R_g and d_{max} values, whereas the two peptides containing KAW10 peptides have significantly smaller R_g and d_{max} values.

Guinier plots for each the four biomaterials show a "roll-over" in the low-Q region; that is, the data begin to fall off with decreasing Q at Q^2 values <0.0001 Å^{-2}. This effect is characteristic of highly asymmetric particles, such as a fiber whose length is much greater than its cross-sectional radius (Figure 5A). The point at which this roll-over begins depends on the aspect ratio ($A = L/2R$, L is the length of the fiber rod and R is the radius of cross-section of the fiber rod) of the rod-shaped fibers; that is, the higher the aspect ratio, the lower the value of Q at which the roll-over begins.[24] A higher aspect ratio means longer fibers with respect to their cross sections. On the basis of the positions of the roll-over points presented in Figure 5A, EAW15:KAW15, EAW10:KAW15, and EAW15:KAW10 pairs all had higher aspect ratio than the EAW10:KAW10 pair. This result implies that the EAW10:KAW10 pair forms the fibers that have the shortest persistence length among the four oligopeptide pairs. None of the four peptide pairs showed a single linear Guinier

(21) Baeucage, G. *J. Appl. Crystallogr.* **1996**, *29*, 134−146.
(22) Beaucage, G. *Phys. Rev. E: Stat., Nonlinear, Soft Matter Phys*, **2004**, *70*, 031401.
(23) Kishimoto, A.; Hasegawa, K.; Suzuki, H.; Taguchi, H.; Namba, K.; Yoshida, M. *Biochem. Biophys. Res. Commun.* **2004**, *315*, 739−745.
(24) Susnick, T.; Charles, S.; Stubbs, G.; Yau, P.; Bradburgy, E. M.; Timmins, P.; Trewhella, J. *Biophys. J.* **1991**, *60*, 1178−1189.

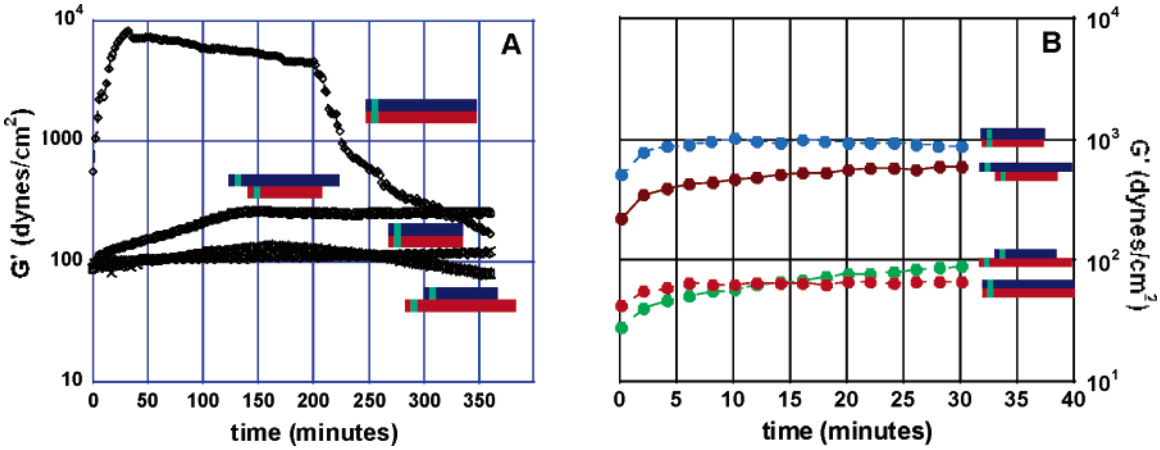

Figure 2. (a) Dynamic time sweep measurement of the initial gelation measured at 0.2% strain amplitude and 1 rad/s angular frequency. (b) Elastic modulus of 23rd gelation (midpoint of cycles 13−32 of repeated shear-induced breakdown recovery cycles). The total peptide concentration was 0.25 wt %. Positive and negative modules were mixed at an equal molar ratio.

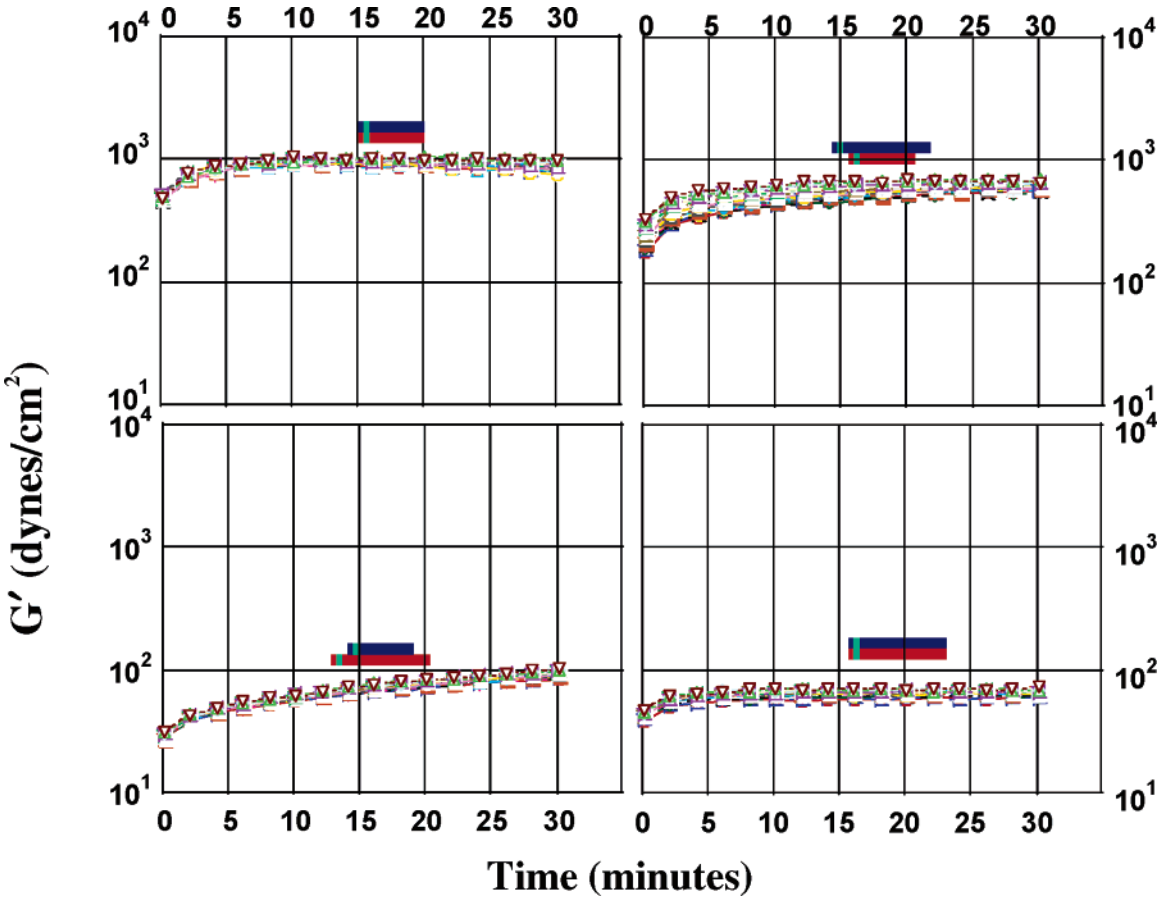

Figure 3. Overlay of recovery profiles from repeated shear-induced breakdowns (200% strain). Shown here are recovery profiles of the 13th−32nd breakdown−recovery cycles.

region for elongated or rodlike particles; rather, there were several linear regions that were indicative of radii of gyration of cross-section (R_c) values in the range 80−170 Å for the EAW15:KAW15 and EAW10:KAW15 pair, and in the smaller range 40−100 Å for the EAW15:KAW10 and EAW10:KAW10 pair. The 30 nm (300 Å) dimension identified in the TEM figures would give rise to an R_c value of ∼106 Å, which is in the range of R_c values seen for peptide pairs with SAXS. Noting that the samples used for TEM and SAXS have very different hydration levels, this behavior is analogous to that of cross-β structures, whose structural features are not affected by the hydration level of the sample.[25]

Semiordered nanostructures, with a repeating mass unit, can be analyzed using mass-fractal power-law decay analysis to explore their morphological characteristics.[21] The Guinier regime probes long-range order that dominates in the low Q

(25) Squires, A. M.; Devlin, G. L.; Gras, S. L.; Tickler, A. K.; Macphee, C. E.; Dobson, C. M. *J. Am. Chem. Soc.* **2006**, *128*, 11738−11739.

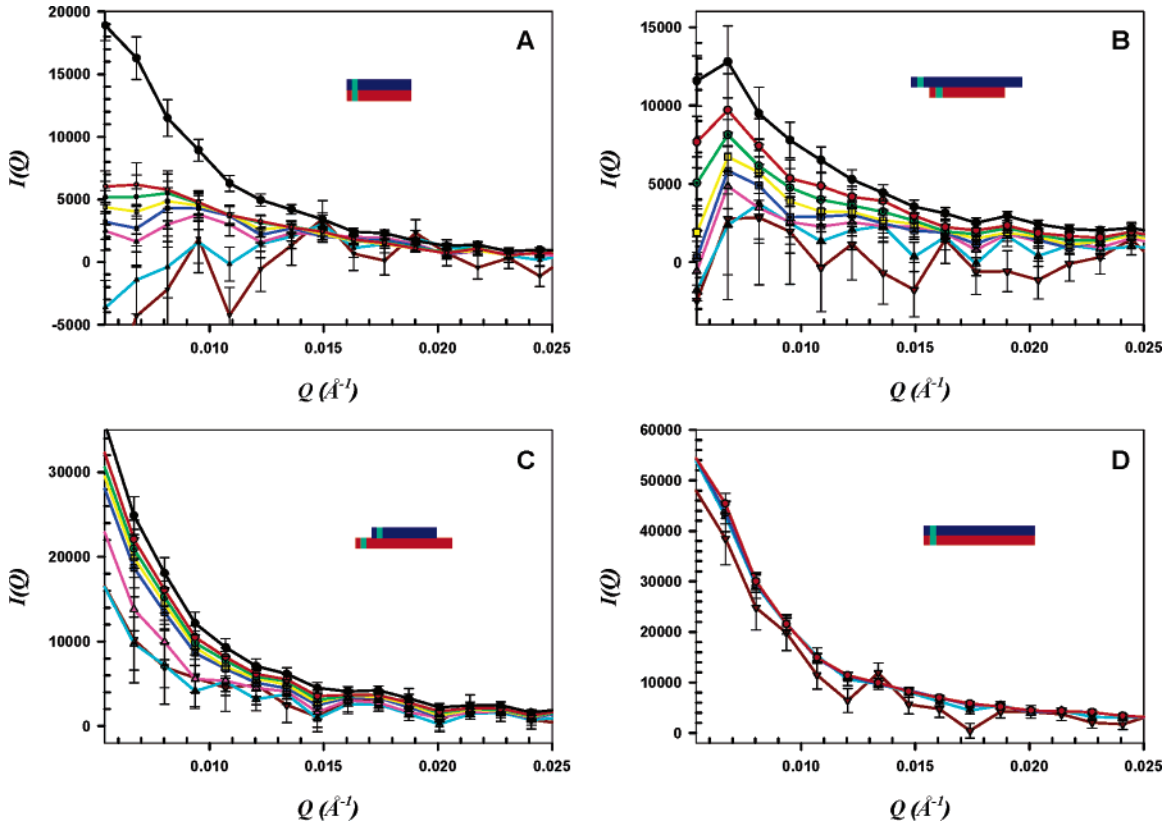

Figure 4. Time evolution of $I(Q)$ vs Q during the process of co-assembly. 15 min, brown inverted triangle; 1 h, light blue crossed triangle; 3 h, pink triangle; 5 h, dark blue crossed square; 7 h, yellow square; 9 h, green crossed circle; 11 h, red circle; 24 h, black circle. $I(Q)$ data are in arbitrary units and on a relative scale.

Table 2. Pairwise Vector Length Distribution Function ($P(r)$) of All Four of the Biomaterials

	R_g[a] (Å)		d_{max}[a] (Å)	
peptide pairs	11 h	24 h	11 h	24 h
EAW15:KAW15	257 ± 10	[b]	750	[b]
EAW10:KAW15	268 ± 26	264 ± 24	750	750
EAW15:KAW10	159 ± 11	170 ± 10	410	450
EAW10:KAW10	150 ± 15	212 ± 25	420	650

[a] R_g is the radius of gyration and d_{max} is the maximum linear dimension of the hydrogels obtained from $P(r)$ analysis. [b] Because there is no measurable difference in the scattering profiles for EAW15:KAW15 between these time points, only the 11 h results are shown.

region, whereas the power-law regime probes the shorter range order corresponding to higher Q region. Mass-fractal analysis of the scattering data reveals fractal dimensions (i.e., d_f values) between 1.5 and 2.0 (Figure 5B). Because the TEM image (see the Supporting Information) shows fibrous structures, disk shapes can be ruled out for these biomaterials with fractal dimension near 2, and it appears that the fibers assemble as Gaussian-coils or swollen Gaussian coils and as a mixture of these forms (Figure 5B). On the basis of d_f values' deviation from 2, the canonical value for Gaussian coil, the degrees of swollenness have the order EAW15:KAW10 (1.5) > EAW15:KAW15 (1.8) > EAW10:KAW15 (1.9) > EAW10:KAW10 (2.0). Note that only the EAW10:KAW10 pair gives a d_f value equal to what is predicted for a true Gaussian coil (i.e., least degree of swollenness) and also forms the strongest hydrogel, suggesting that the presence of the swollen Gaussian coil components play a role in diminishing the strength of the hydrogel. For these kinds of structures, B_f is proportional to the end-to-end distance of the Gaussian coil. The B_f values follow the same order as the d_f values, but in reverse: EAW15:KAW10 (6.0) > EAW15:KAW15 (4.0) > EAW10:KAW15 (1.6) > EAW10:KAW10 (0.6). A larger B_f value signifies, on the average, a longer fiber. These fractal dimensions of these biomaterials are within the range reported in the literature for other heat-set protein gels.[26]

In summary, the SAXS data indicate that the EAW10:KAW10 peptide pair is the slowest to form nanoscale structures and is the only peptide pair to show characteristics of a true Gaussian coil (with least degree of swollenness) in the fractal analysis. Further, the Gunier plot and B_f values indicate that its fiber structures have the shortest persistence length. Because the blunt-end EAW10:KAW10 pair forms a stronger hydrogel than sticky-end pairs (from rheological analysis), we postulate that our hydrogels have nanofibers in which the peptide chains are aligned perpendicular to the fiber axis, as shown in Figure 1. In a previous study,[11] we showed that these oligopeptide fibers bind to the organic dye Congo Red in a fashion similar to that of amyloid fibers.[27] Furthermore, sequences with alternating polar and nonpolar sequence patterns are prone to form fibrillar structures similar to β-amyloid.[28] These features suggest that the structures underlying the oligopeptide fibers are similar to that underlying amyloid fibers, which are cross-β structures. Cross-β structures consist of helical arrays of β-sheets with constitutive β-strands running perpendicular to the helical fiber axis.

(26) Ould Eleya, M. M.; Ko, S.; Gunasekaran, S. *Food Hydrocolloids* **2004**, *18*, 315−323.
(27) Carter, D. B.; Chou, K. C. *Neurobiol. Aging* **1998**, *19*, 37−40.
(28) Broome, B. M.; Hecht, M. H. *J. Mol. Biol.* **2000**, *296*, 961−968.

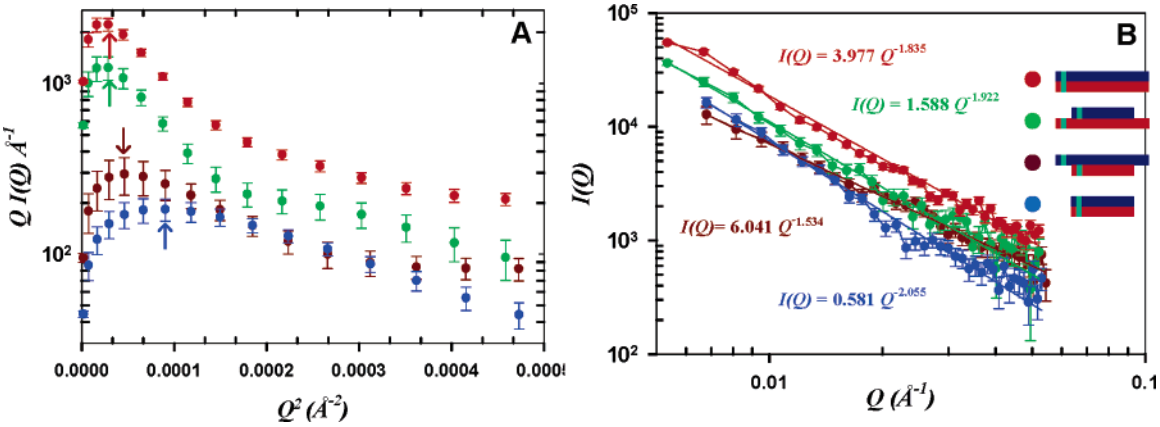

Figure 5. Small-angle X-ray scattering (SAXS) data from each of the four biomaterial at 0.25 wt % total peptide concentration: (A) Guinier plot of the slit-desmeared scattering data for each of the four hydrogels at 24 h (data were desmeared); arrows indicate the rollover points. (B) Log $I(Q)$−Log Q plot to show the mass-fractal, power-law-dependent decay of $I(Q)$ for each coassembled hydrogel (24 h after mixing). $I(Q)$ data are in arbitrary units and on a relative scale.

In addition to demonstrating that sticky ends provide no advantage in terms of gel strength, the rheological measurements show that of the two blunt-ended pairs, the shorter EAW10:KAW10 pair forms a stronger gel than the longer EAW15:KAW15 pair. The reason to this is perhaps due to the structural features of β-strands. Most β-sheet structures found in native proteins and amyloid aggregates have a twisted conformation.[29−32] For a stable cross-β sheet that can twist into a fiber, the optimum chain length in each β-strand is reported to be in the range of 8−12 amino acids.[14] This feature is consistent with our result that the EAW10:KAW10 pair forms a stronger gel than the EAW15:KAW15 pair. Note that the longer chain lengths of proteins that form amyloids are accommodated into the fiber with the polypeptide chain folding back onto itself.[33] In our self-repulsive oligopeptide module, such folding will be prevented because of the electrostatic repulsions and limited chain length. The resulting structure might have dangling ends of peptides in the growing fibers, which could affect fibrillogenesis. This study suggests that the optimum oligopeptide chain length for the coassembly of these biomaterials is around 10. Further detailed investigation of the effect of chain length on the coassembly is underway.

The ability to tune bulk material properties through molecular engineering is an important goal of materials science. This work demonstrates that the mechanical properties of nanofiber networks can be tuned by adjusting the structures of the constitutive oligopeptides.

Conclusion

By pairing peptide modules of equal and unequal chain length (blunt and sticky ends, respectively), we are able to conclude that sticky ends offer no advantage to material assembly in these types of oligopeptide-based hydrogels. The blunt-end hydrogel assembled from the 10:10 peptide pair forms the strongest gel, and the scattering data showed this peptide pair among the four had distinctive kinetic and structural features. Our results are consistent with a cross-β structural model in which β-strands are stacked against each other in a parallel fashion to form nanofibers whose axes is perpendicular to individual β-strands. The optimal chain length of oligopeptide modules for such nanofiber network assembly is around 10 amino acid residues.

Acknowledgment. This work is supported by National Institutes of Health under Grant EB004416 (Y.B.Y.) and made use of the X-ray scattering facilities at the University of Utah that are supported by a grant from the U.S. Department of Energy and in support of the Office of Science/BER Oak Ridge Structural Molecular Biology Center (J.T.). J.T. is supported by an Australian Research Council Federation Fellowship.

Supporting Information Available: Transmission electron microscopic image of EAW15:KAW15 gel (PDF). This material is available free of charge via http://pubs.acs.org.

CM061071L

(29) Wang, J.; Gulich, S.; Bradford, C.; Ramirez-Alvarado, M.; Regan, L. *Structure* **2005**, *13*, 1279−1288.
(30) Sambashivan, S.; Liu, Y.; Sawaya, M. R.; Gingery, M.; Eisenberg, D. *Nature* **2005**, *437*, 266−9.
(31) Sunde, M.; Serpell, L. C.; Bartlam, M.; Fraser, P. E.; Pepys, M. B.; Blake, C. C. *J. Mol. Biol.* **1997**, *273*, 729−739.
(32) Esposito, L.; Pedone, C.; Vitagliano, L. *Proc. Natl. Acad. Sci. U.S.A.* **2006**, *103*, 11533−11538.
(33) Ritter, C.; Maddelein, M. L.; Siemer, A. B.; Luhrs, T.; Ernst, M.; Meier, B. H.; Saupe, S. J.; Riek, R. *Nature* **2005**, *435*, 844−848.